Electronic Supplementary Material (ESI) for ChemComm.
This journal is © The Royal Society of Chemistry 2020

Electronic Supplementary Information (ESI)

In situ sulfidation for controllable hetero-interface engineering of α-$Ni(OH)_2$-Ni_3S_4 hybrid structures realizing robust electrocatalytic methanol oxidation

Changmin Hou, Wenlong Yang, Xianpeng Yang, Bijun Li, Hongtao Gao and Xiliang Luo**

C. M. Hou, Dr. W. L. Yang, X. P. Yang, B. J. Li, Prof. H. T. Gao, Prof. X. L. Luo

Key Laboratory of Optic-electric Sensing and Analytical Chemistry for Life Science, MOE,

Key Laboratory of Analytical Chemistry for Life Science in Universities of Shandong,

College of Chemistry and Molecular Engineering,

Qingdao University of Science and Technology,

Qingdao, Shandong, 266042, P. R. China

E-mail: wlyang@qust.edu.cn; xiliangluo@qust.edu.cn

Experimental

Materials

All reagents were of analytical reagent grade, purchased from Sinopharm Chemical Reagent Co., Ltd., and used as received without further purification.

Synthesis of ultrathin α-$Ni(OH)_2$ nanosheets

Typically, 1 mmol $NiCl_2 \cdot 6H_2O$ and 0.5 mmol ammonium persulfate were dissolved in 200 mL water under vigorous magnetic stirring to form a transparent solution. Then, 1 mL of 28% ammonia solution was added into the above solution drop by drop with vigorous stirring at room temperature. After vigorous magnetic stirring for several minutes, the obtained product was collected by centrifugation and then washed with distilled water and ethanol for several times, and then dried at 60 ^oC in air overnight for further characterization.

Synthesis of α-$Ni(OH)_2$-Ni_3S_4 hybrid structures

In a typical experiment, 50 mg as-obtained ultrathin α-$Ni(OH)_2$ nanosheets and a predetermined amount of thioacetamide (TAA) were dissolved in 50 mL ethylene glycol under vigorous sonication in a 100 mL three neck flask. Then, the above mixture was treated under microwave irradiation in a microwave refluxing system at 140 ^oC for 30 minutes (600 W). After that, the obtained product was collected by centrifugation and washed with distilled water and ethanol for several times, followed by drying at 60 ^oC overnight for further characterization.

Characterization

Powder X-ray diffraction patterns (XRD) were achieved on Japan Rigaku D/max-rA equipped with graphite monochromatized high-intensity Cu Kα radiation (λ = 1.54178 Å). The transmission electron microscopy (TEM) and high-resolution transmission electron microscopy (HRTEM) images were obtained on a JEOL-2010 TEM at an acceleration voltage of 200 kV. The high-angle annular dark-field scanning transmission electron microscopy (HAADF-STEM) and corresponding energy-dispersive spectroscopy (EDS) mapping analyses were performed on a JEOL JEM-ARF200F TEM/STEM. X-ray photoelectron spectroscopy (XPS) valence spectra were recorded on an ESCALAB MKII X-ray photoelectron spectrometer with an excitation source of Mg Kα = 1253.6 eV.

Electrochemical measurements

All electrochemical measurements were carried out in a three-electrode system on an electrochemical station (CHI660B) by using Ag/AgCl (3.3 M KCl) electrode as the reference electrode, a platinum wire as the counter electrode and a glassy carbon electrode with various catalysts as the working electrode. Typically, 4 mg catalysts and 30 μL of 5 wt % Nafion solutions (Sigma-Aldrich) were dispersed in 1 mL water-isopropanol solution with volume ratio of 3:1 under vigorous sonication to form a homogeneous dispersion. Then, 5 μL of the above dispersion was load onto a glassy carbon electrode with a diameter of 3 mm (loading 0.285 mg cm^{-2}). Cyclic voltammetry (CV) was carried out at a scan rate of 50 mV s^{-1} in 1 M KOH solution without and with 0.5 M methanol. Electrochemical impedance spectroscopy (EIS) measurement was performed in 1 M KOH solution, and the frequency

range was 100 kHz to 1 Hz. Chronoamperometric measurement was carried out in 1 M KOH solution containing 0.5 M methanol at a constant potential of 0.45 V vs. Ag/AgCl.

Calculation method

All calculations were performed by using the well tested by the tool of Vienna ab initio simulation package (VASP), which employed plane wave basis sets to treat valence electrons and norm-conserving pseudopotentials to approximate the potential field of ionic cores.[1] We employed generalized gradient approximation (GGA), the Perdew-Burke-Ernzerhof (PBE) exchange–correlation functional, and the ultrasoft pseudopotential in the calculations.[2] During the structural optimization, the cutoff energy was set to be 400 eV, and structure relaxation was performed until the convergence criteria of energy and force reached 1×10^{-5} eV and 0.05 eV•$Å^{-1}$, respectively. Further increasing the cutoff energy brought minor difference in the calculation results. Monkhorst-Pack mesh of 2×2×1 and 4×4×1 k-points were used to sample the two-dimensional Brillouin zone for geometry optimization and electronic structure calculation, respectively. The formation energy (∆E) of γ-NiOOH from α-$Ni(OH)_2$ under alkaline condition (pH = 14) could described as follow equation: $\Delta E = E(NiOOH) + H_2O + E(e^-) - E(Ni(OH)_2) - OH^- = E(NiOOH) + E(e^-) + E(H^+) - E(Ni(OH)_2) = E(NiOOH) + (E(H_2) + 0.059 * pH) - E(Ni(OH)_2)$, where E(system) was the calculated energy of 'system' by DFT calculations.

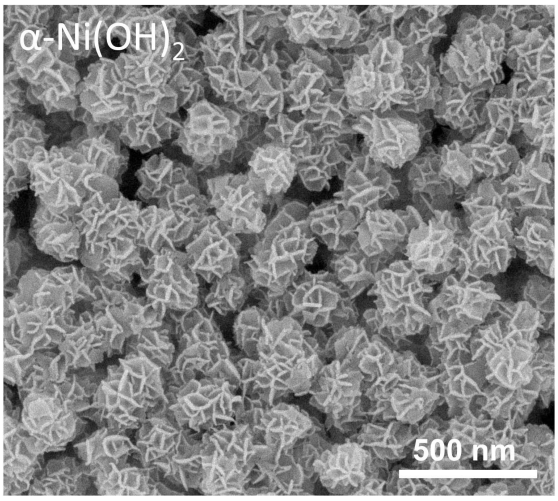

Fig. S1 SEM image of pure α-$Ni(OH)_2$ nanosheets.

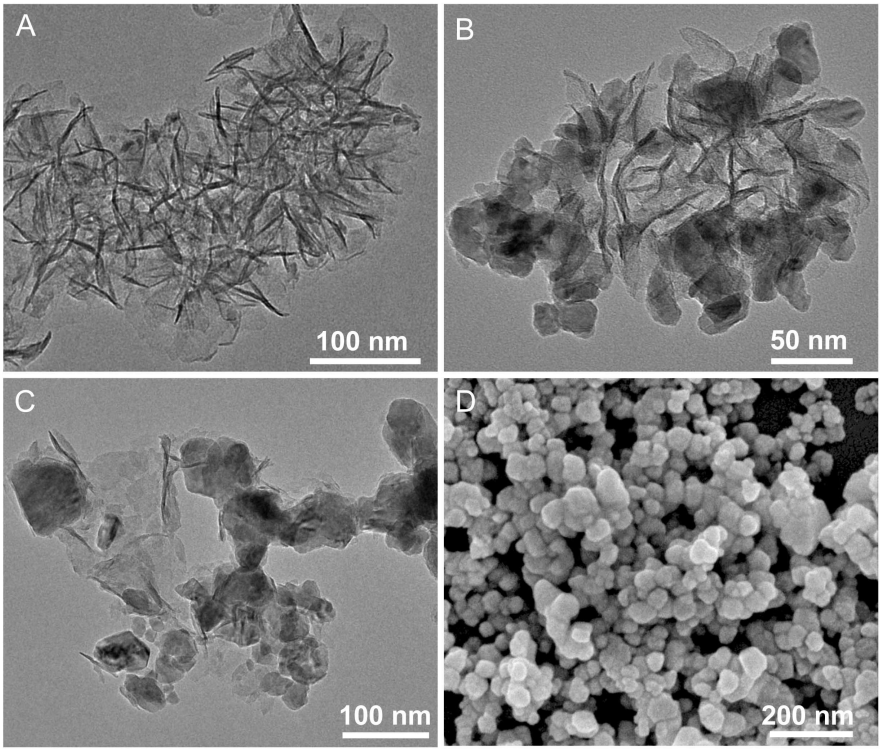

Fig. S2 (A-C) TEM images of HS-1, HS-3 and HS-4 samples, respectively. (D) SEM image of HS-5 sample.

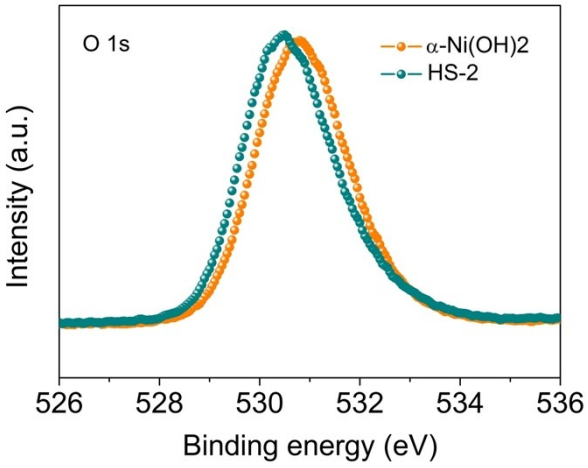

Fig. S3 O 1 s XPS spectra for HS-2 and pure α-Ni(OH)$_2$.

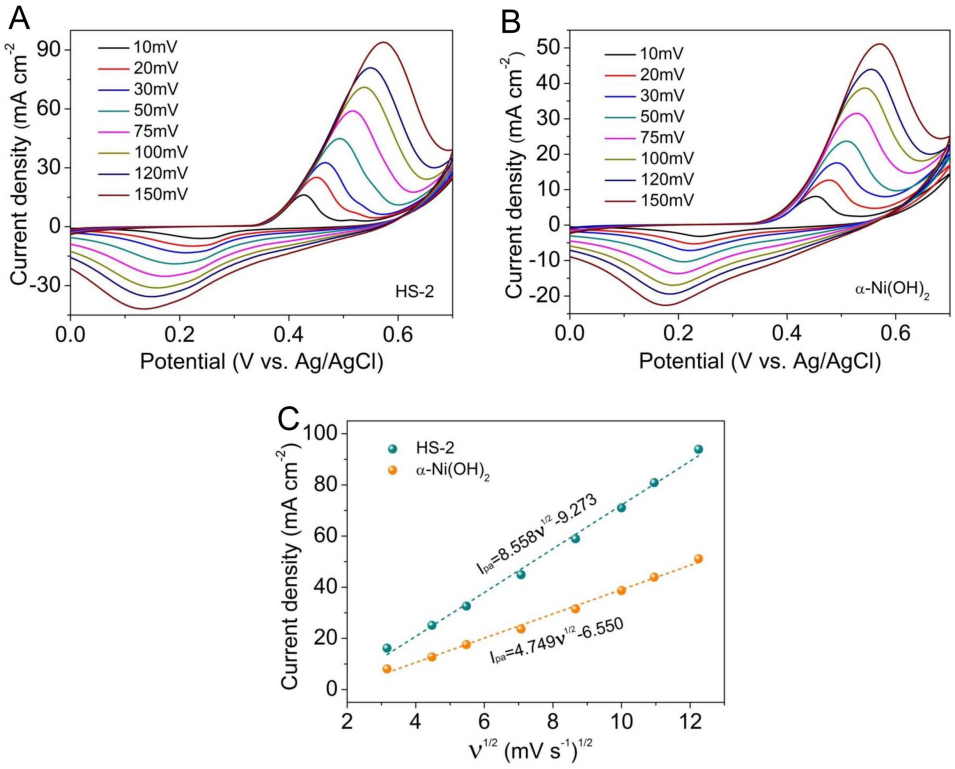

Fig. S4 CV curves of (A) HS-2 and (B) pure α-Ni(OH)$_2$ at different scan rates of 10, 20, 50, 75, 100, 120 and 150 mV s^{-1} in 1 M KOH solution. (C) Corresponding linear relationship between the anodic peak current and the square root of the scan rate ($I_{pa} \sim v^{1/2}$).

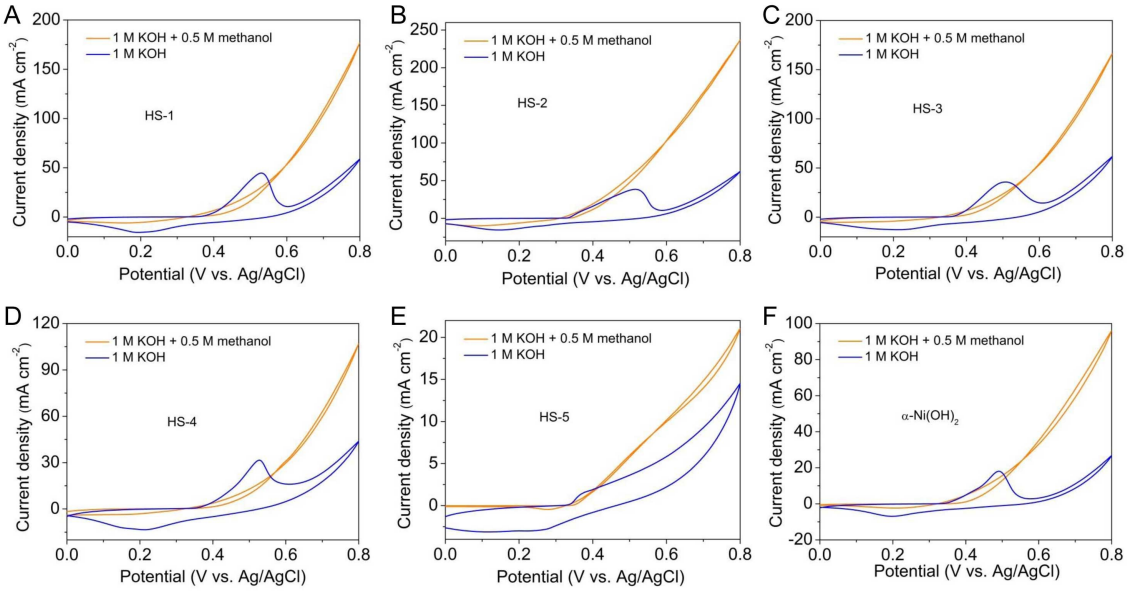

Fig. S5 CV curves of various α-$Ni(OH)_2$-Ni_3S_4 hybrid structures and pure α-$Ni(OH)_2$ measured at a scan rate of 50 mV s^{-1} in 1 M KOH solution with and without 0.5 M methanol.

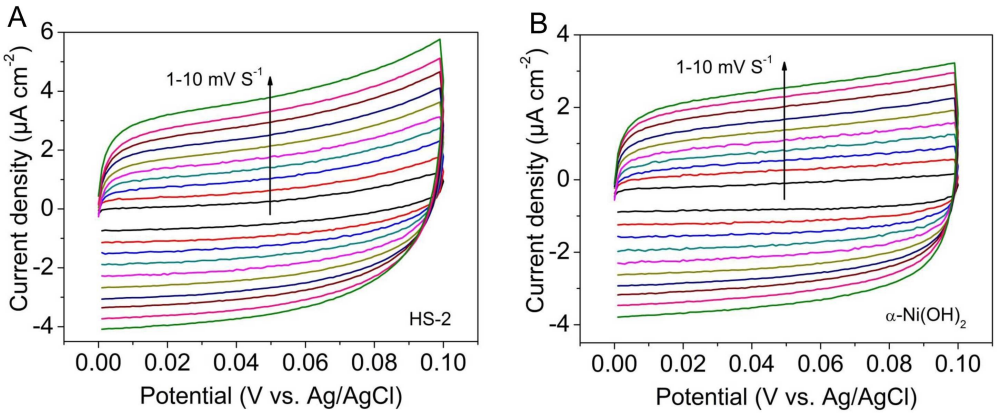

Fig. S6 CV curves of (A) HS-2 and (B) pure α-$Ni(OH)_2$ measured at scan rates from 1 to 10 mV s^{-1} in 1 M KOH solution.

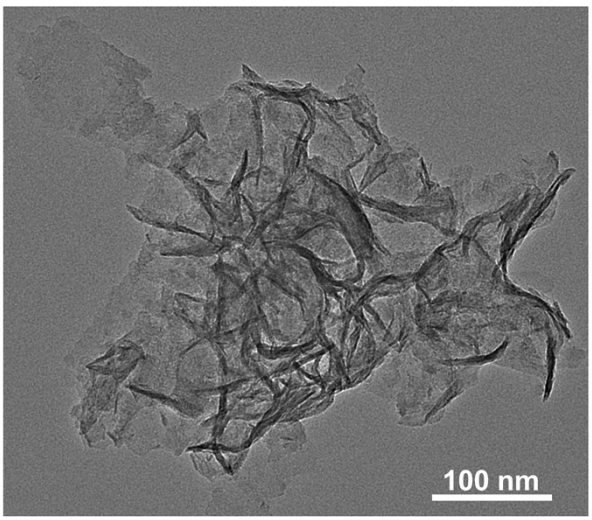

Fig. S7 TEM image of HS-2 after chronoamperometry test in 1 M KOH solution containing 0.5 M methanol.

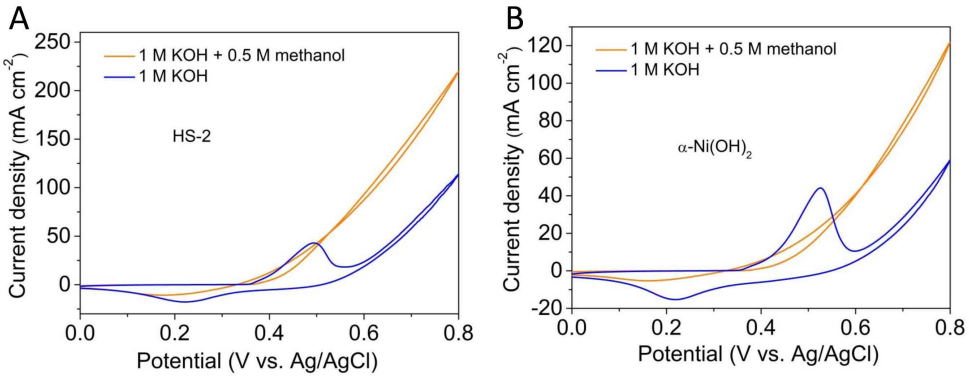

Fig. S8 CV curves of (A) HS-2 and (B) pure α-$Ni(OH)_2$ measured at a scan rate of 50 mV s^{-1} in 1 M KOH solution with and without 0.5 M methanol by using glassy carbon electrode with a diameter of 3mm as the counter electrode.

In order to eliminate the adverse effect of noble metals on MOR, the electrocatalytic MOR activity of pure α-$Ni(OH)_2$ and HS-2 were repeated by replacing glassy carbon electrode (3mm diameter) to Pt counter electrode while keeping other operations unchanged, since minute amounts of noble metals can be dissolved into the electrolyte and then deposited on the pristine catalysts during the electrocatalytic process.[13-15] As shown in Fig. S8, the electrocatalytic MOR activity of HS-2 is higher than that of pure α-$Ni(OH)_2$, which is in accordance with the present result. Of note, compared to the CV curves in Fig. S5, slight changes in anodic current density can be observed, which rules out the potential influence of Pt counter electrode on the electrocatalytic MOR activity.

Table S1 Comparison of the electrocatalytic MOR activity between the HS-2 sample and other recently reported catalysts.

Catalyst	Current density/mA cm^{-2}	Potential/V vs. RHE	Electrolyte	Scan rate/mV s^{-1}
α-$Ni(OH)_2$-Ni_3S_4 hybrid structures, this work	236 167 103	1.82 1.72 1.62	1 M KOH + 0.5 M CH_3OH	50
CNT-Ni/SiC-700[3]	~200	1.82	1 M KOH + 1 M CH_3OH	50
Cu60Ni40@rGO[4]	~190	1.82	1 M KOH + 1 M CH_3OH	100
Ni-Cu alloys [5]	~140	1.82	1 M NaOH + 0.5 M CH_3OH	50
NiO/CNTs[6]	~142	1.62	1 M KOH + 0.5 M CH_3OH	50
NiO nanosheets[7]	~85	1.72	1 M KOH + 0.5 M CH_3OH	50
NiCo bimetallic alloy[8]	~59	1.72	1 M NaOH + 0.5 M CH_3OH	50
Fe-Ni NPs[9]	~50	1.6	1 M NaOH + 1 M CH_3OH	20
Meso NiPO NS[10]	~45	1.7	0.5 M KOH + 0.5 M CH_3OH	50
β-$Ni(OH)_2$-$NiCo_2O_4$[11]	~30	1.67	0.1 M NaOH + 1 M CH_3OH	50
Anodic NiO[12]	~65	1.75	0.1 M NaOH + 1 M CH_3OH	50

Table S2 The DFT data for the formation energy of β-NiOOH.

Species	Energy (Ha)	Energy (eV)	Formation energy (eV)
α-$Ni(OH)_2$-Ni_3S_4 γ-NiOOH-Ni_3S_4	-24869.20 -24858.54	-676740.64 -676450.54	1.40
α-$Ni(OH)_2$ γ-NiOOH	-5887.23 -5876.26	-160203.26 -159904.89	2.32
H_2	-1.16	-31.66	--

Table S3 The DFT data for the adsorption of methanol on the catalyst surface.

Species	Energy (Ha)	Energy (eV)	Adsorption energy (eV)
α-$Ni(OH)_2$-Ni_3S_4	-24869.20	-676740.64	-3.32
α-$Ni(OH)_2$-Ni_3S_4-CH_3OH	-24973.95	-679591.05	
α-$Ni(OH)_2$	-5887.23	-160203.26	-1.47
α-$Ni(OH)_2$-CH_3OH	-5991.91	-163051.82	
CH_3OH	-104.63	-2847.09	--

References

[1] J. Hafner, *J. Comput. Chem.*, **2008**, **29**, 2044-2078.

[2] J. Perdew, K. Burke, M. Ernzerhof, *Phys. Rev. Lett.*, **1998**, *80*, 891.

[3] S. Xie, X. L. Tong, G. Q. Jin,Y. Qin, X. Y. Guo, *J. Mater. Chem. A* **2013**, *1*, 2104-2109.

[4] D. C. Sesu, I. Patil, M. Lokanathan, H. Parse, P. Marbaniang, B. Kakade, *ACS Sustainable Chem. Eng.* **2018**, *6*, 2062-2068.

[5] X. Cui, P. Xiao, J. Wang, M. Zhou, W. L. Guo, Y. Yang, Y. J. He, Z. W. Wang, Y. K. Yang, Y. H. Zhang, Z. Q. Lin, *Angew. Chem. Int. Ed.* **2017**, *56*, 4488-4493.

[6] X. L. Tong, Y. Qin, X. Y. Guo, O. Moutanabbir, X. Y. Ao, E. Pippel, L. B. Zhang, M. Knez, *Small* **2012**, *8*, 3390-3395.

[7] W. L. Yang, X. P. Yang, J. Jia, C. M. Hou, H. T. Gao, Y. N. Mao, C. Wang, J. H. Lin, X. L. Luo, *Applied Catalysis B: Environmental* **2019**, *244*, 1096-1102.

[8] X. Cui, W. L. Guo, M. Zhou, Y. Yang, Y. H. Li, P. Xiao, Y. H. Zhang, X. X. Zhang, *ACS Appl. Mater. Interfaces* **2015**, *7*, 493-503.

[9] S. L. Candelaria, N. M. Bedford, T. J. Woehl, N. S. Rentz, A. R. Showalter, S. Pylypenko, B. A. Bunker, S. Lee, B. Reinhart, Y. Ren, S. P. Ertem, E. B. Coughlin, N. A. Sather, J. L. Horan, A. M. Herring, L. F. Greenlee, ACS Catal. 2017, 7, 365-379.

[10] X. Y. Song, Q. Sun, L. Gao, W. Chen, Y. F. Wu, Y. M. Li, L. Q. Mao, J. H. Yang, *Int. J. Hydrogen. Energy.* **2018**, *43*, 12091-12102.

[11] M. U. A. Prathapa, B. Satpati, R. Srivastava, *Electrochim. Acta* **2014**, *130*, 368-380.

[12] L. Y. Wang, G. G. Zhang, Y. Liu, W. F. Li, W. Lu, H. T. Huang, *Nanoscale* **2016**, *8*, 11256-11263.

[13] A. A. Topalov, I. Katsounaros, M. Auinger, S. Cherevko, J. C. Meier, S. O. Klemm, Karl J. J. Mayrhofer, *Angew. Chem. Int. Ed*. **2012**, *51*, 12613-12615.

[14] R. Chen, C, J. Yang, W. Z. Cai, H. Y. Wang, J. W. Miao, L. P. Zhang, S. L. Chen, B. Liu, *ACS Energy Lett.* **2017**, *2*, *5*, 1070-1075.

[15] T. J.P. Hersbach, A. I. Yanson, M. T.M. Koper, *Nature Communications* **2016**, *7*, 12653.